Structural Biology and Molecular Biophysics
Computational and Systems Biology

Discovery of a Heparan Sulfate Binding Domain in Monkeypox Virus H3 as an Anti-poxviral Drug Target Combining AI and MD Simulations

Reviewed Preprint
v2 • December 2, 2024
Revised by authors

Reviewed Preprint
v1 • August 13, 2024

Bin Zheng, Meimei Duan, Yifen Huang, Shangchen Wang, Jun Qiu, Zhuojian Lu, Lichao Liu, Guojin Tang, Lin Cheng, Peng Zheng

State Key Laboratory of Coordination Chemistry, Chemistry and Biomedicine Innovation Center (ChemBIC), School of Chemistry and Chemical Engineering, Nanjing University, Nanjing, China • Institute for Hepatology, National Clinical Research Center for Infectious Disease, Shenzhen Third People's Hospital, Shenzhen, China • Department of Intensive Care Unit, Nanjing Drum Tower Hospital, Affiliated Hospital of Medical School, Nanjing University, Nanjing, China

eLife Assessment

This work presents **important** findings regarding the interaction of the monkeypox virus (MPXV) attachment H3 protein with the cellular receptor heparan sulfate and the use of this information to develop antivirals potentially effective against all orthopoxviruses. Using a combination of state-of-the art computational and wet experiments the authors present **convincing** evidence to sustain their claims. These results will interest those working on basic orthopoxviruses biology and antiviral development.

https://doi.org/10.7554/eLife.100545.2.sa4

Abstract

Viral adhesion to host cells is a critical step in infection for many viruses, including monkeypox virus (MPXV). In MPXV, the H3 protein mediates viral adhesion through its interaction with heparan sulfate (HS), yet the structural details of this interaction have remained elusive. Using AI-based structural prediction tools and molecular dynamics (MD) simulations, we identified a novel, positively charged α-helical domain in H3 that is essential for HS binding. This conserved domain, found across *orthopoxviruses*, was experimentally validated and shown to be critical for viral adhesion, making it an ideal target for antiviral drug development. Targeting this domain, we designed a protein inhibitor, which disrupted the H3-HS interaction, inhibited viral infection *in vitro* and viral replication *in vivo*, offering a promising antiviral candidate. Our findings reveal a novel therapeutic target of MPXV, demonstrating the potential of combination of AI-driven methods and MD simulations to accelerate antiviral drug discovery.

Introduction

The mpox virus (MPXV), a zoonotic pathogen within the *Orthopoxvirus* genus, has emerged as a global health concern. This genus also includes the Variola virus (VARV), the causative agent of smallpox, and Vaccinia virus (VACV), which has been used as a live vaccine against smallpox[1], [2] (**Fig. 1A**). Historically endemic to Central and West Africa, MPXV gained international attention during the global outbreaks in 2022 (clade IIb) and 2024 (clade Ib), leading the World Health Organization (WHO) to declare it a public health emergency of international concern twice within three years[3]-[5]. Although MPXV has a lower fatality rate than smallpox (2-10% versus 30%), the absence of specific antiviral treatments continues to pose significant health risks[6]-[11].

Viral adhesion to host cells is a critical initial step in the infection process for many viruses. Proteins that mediate these interactions have been identified as essential therapeutic targets, offering promising opportunities for antiviral therapies. In *orthopoxviruse*s such as monkeypox virus (MPXV), the H3 protein plays a pivotal role in facilitating viral adhesion by binding to cell-surface heparan sulfate (HS)[12]-[14], a glycosaminoglycan essential for viral entry. H3-specific neutralizing monoclonal antibodies have shown to protective effects for rabbits and immunodeficient mice against lethal poxvirus infections[15]. And H3 is a key component in recent mpox vaccines[16], [17]. Despite the central role of H3 in MPXV infection and protection, the structural details of its specific interaction with HS remain elusive.

Understanding the molecular mechanisms underlying the H3-HS interaction is critical for advancing antiviral drug development. H3 is highly conserved across *poxviruses* (**Fig. 1A**), including variola and vaccinia viruses, making it a potential target for broad-spectrum therapies. The recent resurgence of MPXV infections has underscored the urgent need for specific antiviral treatments. Given the conserved nature of H3 across all known MPXV lineages, including Clade Ib, which has been linked to the 2024 outbreak, designing therapies that target H3 could offer a robust solution to current and future outbreaks.

However, efforts to resolve the complete structure of H3-HS complex, have been hampered by the dynamic and flexible nature of HS and the tendency of H3 self-cleavage. Classic structural biology techniques, such as X-ray crystallography, have been unable to capture the full interaction between H3 and HS due to these complexities. Therefore, alternative approaches are required to fully elucidate this critical interaction.

To address these challenges, we employed advanced AI-based protein structural prediction and generation tools, including AlphaFold2(AF2) and RFdiffusion, alongside classic molecular dynamics (MD) simulations. These state-of-the-art computational techniques enabled us to identify key HS-binding sites within H3 and to characterize the binding mechanisms of the previously uncharacterized α-helical domain[18]-[22]. Corroborated by various experimental methods[23]-[26], the use of AI-driven tools proved pivotal in overcoming the limitations of traditional structural methods, allowing us to predict and validate the structure-function relationship of the H3-HS interaction. A powerful approach for unraveling complex protein-glycan interactions is demonstrated, offering new pathways for the development of broad-spectrum antiviral therapies[27], [28].

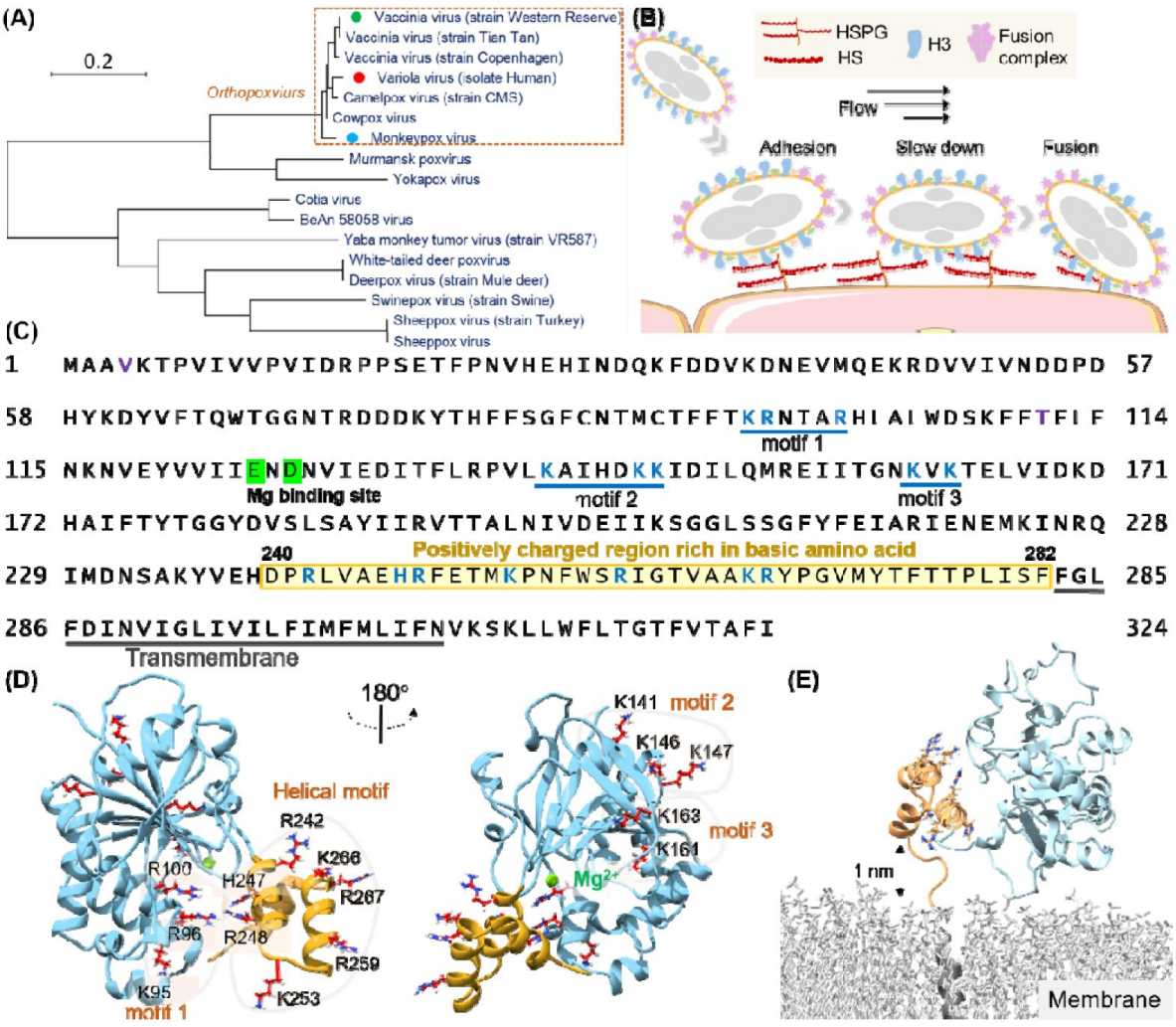

Fig. 1.

Structural Analysis of the H3 Protein in Monkeypox Virus

(A) Phylogenetic tree depicts the evolutionary relationships of H3 within the *Poxviridae* family, highlighting MPXV (blue circle), VARV (red circle), and VACV (green circle). (B) Schematic of MPXV adhesion to the cell surface. Viral particles bind to cell surface via specific interaction such as between adhesion protein H3 and HS, followed by membrane fusion mediated by the fusion complex, allowing entry into the host cell. (C) The amino acid sequence of MPXV H3 shows the newly discovered helical structure (240-282, highlight in yellow), the Mg(II) (green) binding site and other potential HS binding motifs (blue underlines). (D) AF2 prediction of MPXV H3 structure. The left and right panels show different orientations of the H3 structure (rotated 180°). The blue region corresponds to H3(1-239), which has a homologous crystal structure (VACV H3, PDB code: 5EJ0). The yellow region represents the AF2-predicted structure of H3(240-282), which remains unresolved in the crystal structure of the homologous protein. All potential GAGs-binding motifs are highlighted with a yellow background. (E) MD simulation snapshot of H3 on a DPPC membrane. H3 is anchored to the membrane through its transmembrane region (residues 283-306, in gray).

Result

Identification of a Novel Helical Domain for HS Binding in H3

The H3 protein of MPXV is a 324-amino-acid transmembrane protein conserved across all 12 identified *orthopoxviruses*. Previous studies have shown that its extracellular domain (residues 1-282) binds to cell-surface heparan sulfate (HS)[29], [30], facilitating viral entry in conjunction with other adhesion proteins and the fusion protein system (**Fig. 1B**)[31]. Inhibiting the HS binding to H3, therefore, represents a promising strategy for developing broad-spectrum antiviral therapies against *orthopoxviruese*. While most structure of the extracellular region of Vaccinia virus H3 (residues 1-240; PDB code: 5EJ0) has been solved, the dynamic and heterogeneous nature of HS as a biopolymer complicates the identification of precise binding sites.

To identify HS binding sites on the H3 protein, we first performed a comprehensive sequence and structural analysis. As a highly negatively charged glycosaminoglycans, it is believed that HS interacts with positive charge residues on proteins by electrostatic interaction. Previous studies have indicated that the positively charged Mg (II) ion in H3 is critical for HS binding. Therefore, we focused on regions rich in basic amino acids—lysine (K), arginine (R), and histidine (H). Given that only the H3 structure from VACV was available[28], we used AlphaFold2 (AF2) to model the MPXV H3 structure (Fig. S1A), Our analysis revealed three potential HS binding motifs rich in positively charge residues: Motif 1 (K95, R96, R100), Motif 2 (K141, K146, K147), and Motif 3 (K161, K163)[32], all located within the homologous structure of VACV H3 (**Fig. 1C, D**).

Interestingly, we also identified a cluster of seven additional positively charged residues (R242, H247, R248, K253, R259, K266, R267) in the protein C-terminal region. This region had not been previously structurally characterized due to its self-cleavage during sample preparation for X-ray diffraction studies, but was retained in all other biochemical and viral assays[28-30]. AF2 predicted these residues to form a three-helical domain with high confidence (pLDDT score: 82.9 for overall structural; 80.6 for the helical domain, 100 for the maximum score), suggesting it may serve as an HS binding site as a structured domain (**Fig. 1D**). We also tested other models, such as ESMFold (pLDDT:70.6; 50.7) and RoseTTAFold2 (pLDDT: 70.2; 50.7) (Fig. S1B&C) [33], [34]. They all predict a helical structure. But their results are different in detail and had lower confidence scores. Thus, we used AF2 for further studies. Another concern is that the helical domain near the virus surface. Thus, we modeled the complete structure of H3 in virus using a model DPPC (dipalmitoylphosphatidylcholine) membrane. It showed a dynamic movement between the helical domain and the membrane, with a maximum distance exceeding 1 nm (**Fig. 1E**, Fig. S1D&E, Supplementary Video 1). Thus, enough space be present for possible HS binding.

Flexible molecular docking and MD simulations identified the exact HS binding sites in the H3 protein.[35], [36]. We used a 20-repeat HS unit with a specific composition for detailed analysis ($[IdoA2S\text{-}GlcNS6S\text{-}IdoA\text{-}GlcNS(3,6S)]_5$) (Fig. S2). A 500 ns MD simulation established the equilibrium conformation of H3, and subsequent docking with AutoDock Vina identified four high-scoring conformations for each motif (**Fig. 2A**, Fig. S3). The docking score calculated by the software reflects the total energy of interactions between molecules. Lower scores (more negative values) indicate more stable binding between the molecules. To address the dynamic nature of HS, we extended our simulations to 3 times additional 1000 ns MD simulations for each conformation. RMSD (Root Mean Square Deviation) analysis demonstrated notably stable binding for HS to both Motif 1 and the newly identified helical domain (Supplementary Video 2), with RMSD values consistently below 4 nm, indicating minimal structural fluctuations during interaction (**Fig. 2B**).

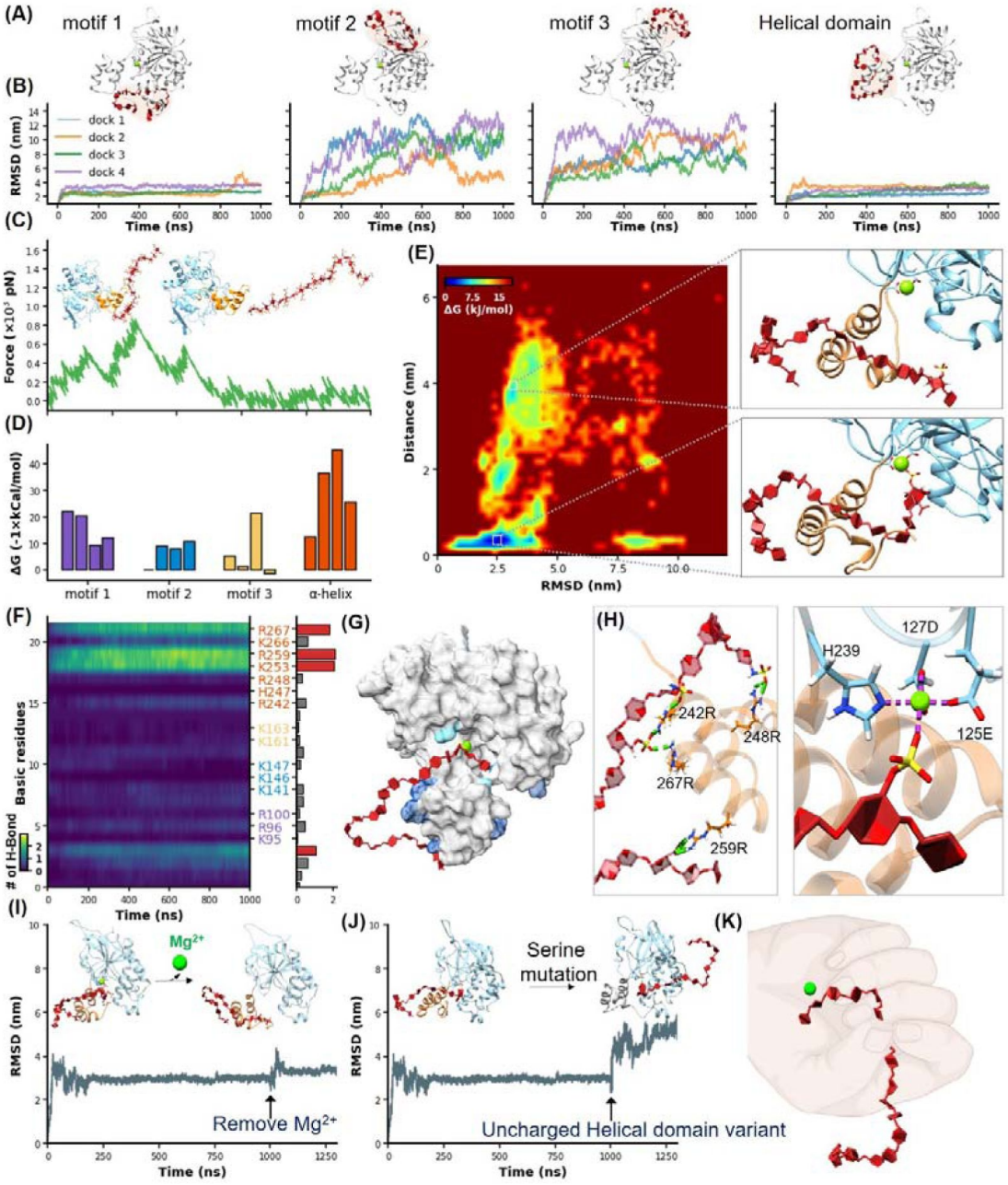

Fig. 2.

Identification of HS Binding Motifs in H3 by MD Simulation and Docking

(A-B) Cartoons show docking results of HS with Motifs 1, 2, 3, and the helical domain, respectively. Panels (B) show RMSD values from 1μs MD simulations, color-coded to match the configurations in (A). (C) Schematics illustrates the reaction coordinate in umbrella sampling, highlighting HS dissociation from H3 with a green force curve. (D) Histogram shows the binding free energies for HS-H3 interactions in motifs 1, 2, 3, and the helical domain. (E) A free energy landscape map from a 1000 ns REMD simulation shows HS binding configurations to the helical and Mg(Ⅱ) regions. (F) Panel provides salt bridge formation statistics between HS and H3's basic amino acids, with a bar chart of average formations. (G) A surface plot shows the frequency of salt bridge formations within H3, with areas of frequent formations in blue. (H) Detailed views of HS-H3 interactions, with the left image showing salt bridges and the right image displaying electrostatic interactions with Mg(Ⅱ). This panel illustrates the impact on HS binding stability to H3 following the removal of Mg(Ⅱ) during the simulation. (J) The effects of mutating all basic amino acids in the helical domain on the binding stability of HS are shown. (K) The "palm-binding" model is depicted where HS is secured by the helical "fingers" and interacts with the Mg(Ⅱ)-bound "palm.".

Moreover, we quantitatively analyzed the binding free energy between H3 and HS in different conformational states using umbrella sampling (US) techniques. A harmonic potential was applied to HS and gradually pulled away from H3, generating a series of reaction coordinates (**Fig. 2C**, Fig. S4, Supplementary Video 3). The green force-extension curve represents the force during this stretching process. This curve, along with the corresponding PMF (Potential of Mean Force) variation shown in Figure S4, demonstrated the free energy changes throughout the umbrella sampling process, revealing that the helical domain possesses the highest binding affinity with a ΔG of -45 kCal/mol (**Fig. 2D**).

Previous studies have suggested the critical role of the Mg(II) ion in stabilizing HS binding, where its removal reduces binding efficiency[29]. Indeed, the α-helical domain is very close to the Mg(Ⅱ)-bound region in H3. Notably, these two parts appear to form a distinct cavity-like binding pocket for HS (**Fig. 1E**, **Fig. 2E**). Thus, we conducted a 1000 ns REMD (Replica Exchange Molecular Dynamics) simulation of the H3-HS complex to further understand the binding dynamics. REMD, an advanced sampling technique, helps overcome the kinetic barriers typically encountered in conformational transitions by utilizing a series of temperature-controlled replicas to enhance the exploration of the conformational landscape[37]. For this study, we set up 64 replicas over a temperature range from 310K to 387K, cumulatively simulating for 64 μs. This comprehensive simulation captured the HS molecule progressively binding deeper into a cavity formed by the α-helical domain, eventually interacting with the Mg (II) ion as hypothesized (**Fig. 2E**, Supplementary Video 4).

The free energy landscape, mapped out from these simulations, shows HS transitioning from a stable interaction with the helical domain across an energy barrier into the Mg (II)-enhanced cavity. This dual interaction—first with the helical domain and then with the Mg(II) site—was consistently observed to stabilize the complex further, evidenced by a significantly lower binding free energy of -67 kCal/mol (Fig. S4)[38]. These results underscore the dynamic nature of the H3-HS interaction and validate our model of sequential binding, which could be critical for designing inhibitors that target these specific interactions.

Given the crucial role of electrostatic interactions in the HS-H3 binding process, we conducted an exhaustive analysis of salt bridge formations across all MD simulation trajectories. This analysis focused on the formation of salt bridges over time between the basic amino acids (R, K, H) of H3 and HS, with brighter areas indicating more frequent formation of salt bridges and robust interaction (**Fig. 2F**, Fig. S5). A bar graph accompanied these maps, quantifying the average number of salt bridges each amino acid formed during the simulations, further illustrating the intensity and frequency of these interactions. Our findings demonstrated a high affinity of HS for the helical domain of H3, with basic amino acids in this region forming more salt bridges compared to other parts of the protein. The surface hotspot map of H3 (**Fig. 2G**) visually highlighted these interactions, with varying shades of blue representing the frequency of salt bridge formation, emphasizing their distribution and intensity. In the helical domain, a focus view showed that the 1st, 7th, 9th, and 18th sugar units of HS formed salt bridges with R248, R242, R267, and R259 of H3, respectively (**Fig. 2H**, left), while the sulfate group on the 2nd sugar side chain of HS bound to Mg(II) (**Fig. 2H**, right).

To further prove these findings, we performed two control experiments. First, we removed the Mg(Ⅱ) ion during MD simulation. According to the results of umbrella sampling, we extended the simulation of the most stable H3-HS binding conformation to 1000 ns, then removed the Mg(Ⅱ) ion and continued the simulations. The resulting increase in RMSD fluctuations confirmed the stabilizing role of Mg(Ⅱ) in the binding process (**Fig. 2I**, Supplementary Video 5). Second, we mutated all seven positively charged amino acids in the helical domain to serine, and name it H3 (uncharged). While AF2 predicted that the helical structure would remain intact (Fig. S6), a significant alteration in HS binding dynamics was observed, supporting the critical role of these charged residues in stabilizing the interaction (**Fig. 2J**, Supplementary Video 6).

Our interaction model revealed that the α-helical domain of H3 functions like a thumb, guiding HS into a stable binding position, while the Mg(II) region acts like a palm, securing HS in place. This dynamic interaction allows HS to transition from an initial surface-level binding to being deeply anchored within the protein cavity, illustrating a complex yet well-organized binding process (**Fig. 2K**).

Bioinformatic analysis of the H3 protein across the *Poxviridae* family highlights its evolutionary conservation and its significance in HS binding. Given the crucial role of electrostatic interactions in the H3-HS binding process, we analyzed the charge distribution within the helical domain. To date, H3 proteins have been discovered in 66 of 118 known *Poxviridae* species. Using NCBI's BLAST, we retrieved sequences of these 66 H3 proteins and performed multiple sequence aligment[39]. A heatmap detailing the side-chain charge distribution at a physiological pH of 6.5—mimicking the microenvironment of H3-HS interaction—revealed a significant concentration of positive charges at the helical domain (**Fig. 3A**). Furthermore, structural predictions using AF2 showed that all these 66 sequences generally share a similar architecture to MPXV H3, particularly in the presence of the α-helical domain (Fig. S7).

Notably, this domain consistently exhibited an accumulation of basic amino acids such as lysine, arginine, and histidine, which are essential for binding the negatively charged HS. These amino acids, including residues identified as 358, 361, 367, 373, 379, 386, and 387 in *Poxviridae* H3 (global position in alignment), corresponding to residues H239, R242, R248, K253, R259, K266, R267 in MPXV H3, show high conservation (**Fig. 3B**, Fig. S8). Surface charge analysis of H3 proteins from four *orthopoxviruses*, including MPXV, VACV, VARV, and CPXV confirmed the predominance of strong positive charges in their α-helical domains (**Fig. 3C**), crucial for effective binding to HS. This consistent feature across different viruses underscores the evolutionary importance of the helical domain, suggesting a universal mechanism in orthopoxviral adhesion that could be targeted in antiviral strategy.

Experimental Confirmation of the Structure and Function of α-Helical Domain

To validate the computational predictions, we first conducted experiments using atomic force microscopy-based single-molecule force spectroscopy (AFM-SMFS). This technique, widely used for studying protein (un)folding, allowed us to directly assess the structure and stability of the α-helical domain within the H3 protein[40-42]. We engineered the H3 construct with two GB1 domains, each 18 nm in length upon unfolding, and one Cohesin module for precise measurement (**Fig. 3D**)[43-45]. These proteins are immobilized on the surface by click chemistry and enzymatic ligations (Fig. S9)[46-48]. During the experiment, the coated AFM tip with GB1 and Dockerin initiated a Coh-Doc interaction, producing a characteristic sawtooth-like force-extension curve as it was stretched (**Fig. 3D&E**). Notably, two peaks corresponding to the unfolding of the α-helical domain were observed. The first peak showed a contour length increment (ΔLc) of 13 nm, closely matching the theoretical unfolding length for the 42 amino acid-long α-helical domain of H3 (residue 240-282, 42aa*0.36 nm/aa-2.6 nm)[49]. The measured unfolding force was 67.4 ± 2.1 pN (mean ± SEM, *n*=139), while the second peak indicated the unfolding of the remaining structure of H3, with a ΔLc of 84 nm (**Fig. 3F**). The total unfolding, represented by a cumulative ΔLc of 97 nm, confirmed the structured and stable nature of the α-helical domain within H3.

We further explored the functional role of the α-helical domain in mediating H3's binding to HS using AFM on live cells[50, 51]. The H3 protein was linked to the AFM tip and approached cultured CHO-K1 cells, which express HS, mounted on a Petri dish. Inverted microscopy was used to precisely control the positioning of the AFM tip. Upon contact, the interaction between H3 and HS was initiated, and the binding event was monitored by retracting the tip to generate a force-extension curve. A distinct peak, corresponding to H3-HS interaction, was observed with a dissociation force of 33.7 ± 0.2 pN and a binding probability of 43% (**Fig. 4A, B**). Repeated trials

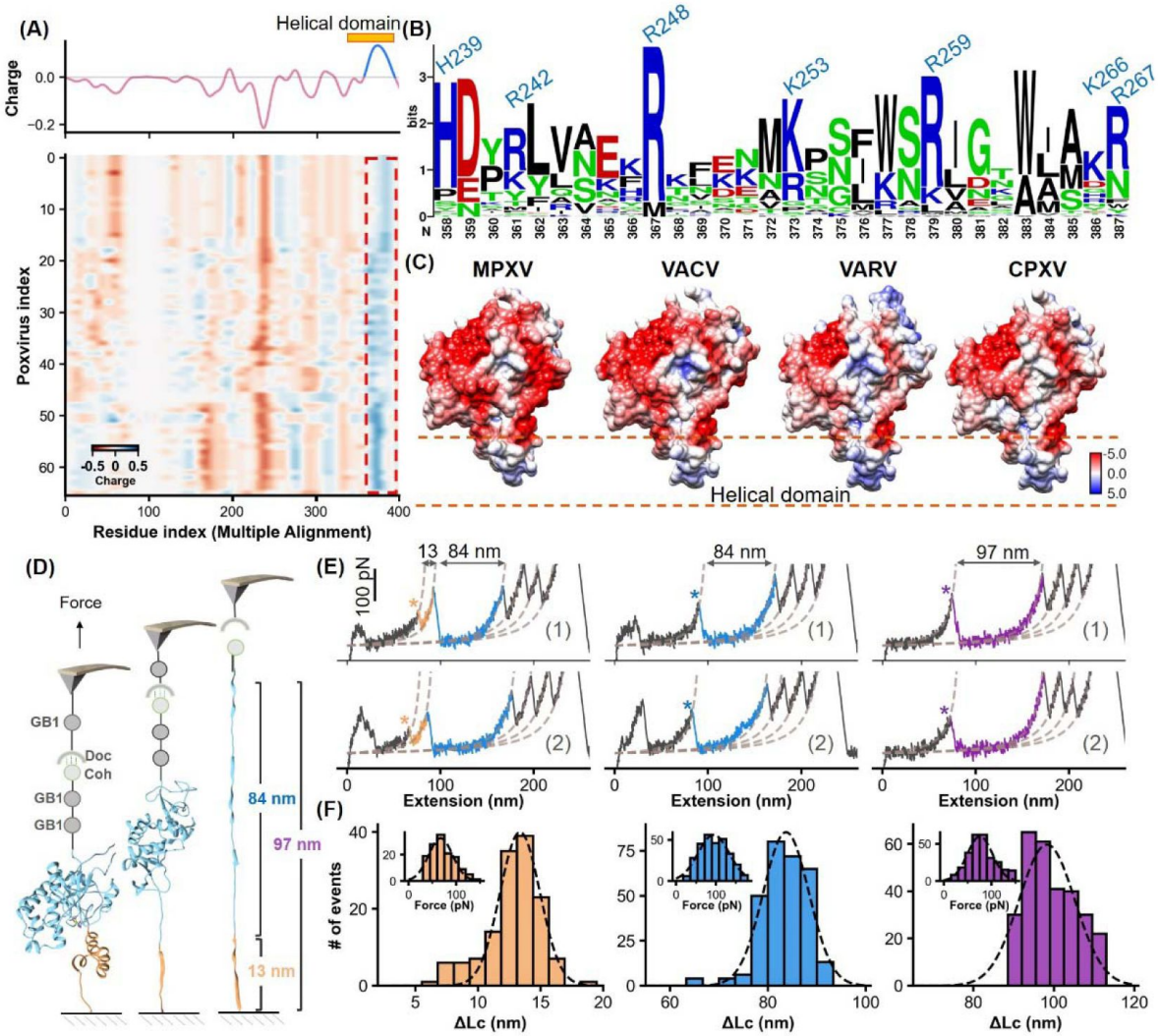

Fig. 3.

Charge Characteristics and Structural Analysis of H3 Protein

(A) The heatmap shows the amino acid charge distribution in the H3 protein across 66 *Poxviridae* viruses, following multiple sequence alignment. Blue indicates areas with more positive charges, and red indicates more negative charges. The accompanying curve shows the average charge of all amino acids in *Poxviridae* H3. (B) Logo plot of the amino acid sequence of the helical region, highlighting the conservation of basic amino acids at specific positions. (C) The surface charge analysis of H3 from the MPXV, VACV, VARV, and cowpox viruses (CPXV) with the helical domain showing a significantly positive charge. (D) Schematic of the single-molecule force spectroscopy unfolding experiment on H3, illustrating the unfolding process of the helical domain (yellow) followed by the main body (blue). (E) Representative curves of H3 unfolding, color-coded to show the helical region (yellow), main body (blue), and full-length (purple) unfolding. (F) Histograms depict the force spectroscopy signals for helical domain, main body, and full-length unfolding, with ΔLc statistics provided. The inset shows a Gaussian fit of unfolding forces.

across different cell surface areas produced a detailed force map, quantifying the distribution of HS unbinding forces and further confirming the critical role of the helical domain in viral adhesion (**Fig. 4C, D**).

Moreover, we performed mutagenesis studies on the α-helical domain by replacing all positively charged residues with serine. AFM experiments on this variant H3(uncharged) showed a detectable force peak with a lower unbinding force of 28.8 ± 0.2 pN, compared to 33.7 ± 0.3 pN for the wild type—representing a 14% reduction (ΔForce > 2*SEM, 95% CI)—and a significant decreased HS binding probability from 43% to 25% (**Fig. 4C, D**). These results suggest that the basic amino acids in the helical domain are crucial for HS binding. To confirm the specificity of the interaction, CHO-K1 cells were treated with heparinase II, an enzyme that degrades HS. This treatment further reduced the dissociation force to 23.0 pN and the binding probability to 12.6%, confirming that the observed interactions were specific to the HS-H3 complex.

Further validation was carried out using flow cytometry (FCM). We fused eGFP, a fluorescent reporter protein, to the C-terminus of both the H3(WT) and the H3(uncharged). Following incubation of these fusion proteins with cells, FCM analysis showed a significant reduction in mean fluorescence intensity in cells treated with H3(uncharged) compared to H3(WT) (**Fig. 4E**). Statistical analysis of multiple experiments highlighted a significant difference between the two (**Fig. 4F**). These findings, along with the results from MD simulations and AFM force spectroscopy, underscore the importance of the positively charged amino acids in the α-helical domain of H3 for efficient HS binding.

The Helical Domain Serves as a Target for H3 Infection Inhibition

Targeting the α-helical domain of H3 as H3 binding sites, we *de novo* designed a series of inhibitors. Using deep-learning model RFdiffusion, we designed a series of inhibitors for the H3-HS interaction and named it AI-PoxBlock (**Fig. 5A**). Sequence recovery for each series was performed on 1000 backbones using ProteinMPNN, generating ten sequences per backbone. These designs were further validated through complex structure predictions using AF2-multimer, and candidates were selected based on PAE (Predicted Aligned Error) values below 7 and iPTM (interface predicted Template Modelling) scores above 0.9. The predicted structures of these candidates also exhibited RMSD values of less than 2 nm when compared to the RFdiffusion-generated structures (Fig. S10). To assess the binding capabilities of these inhibitors, we conducted 500 ns MD simulations, analyzing RMSD trajectories. Five inhibitors—AI-PoxBlock302, 602, 614, 723, and 761—demonstrated stable RMSD values under 0.4 nm, confirming their potential for stable binding to the helical domain of H3 (Fig. S11, S12, Supplementary Video 7).

Although AI-PoxBlock302 could not be successfully expressed, the remaining four inhibitors underwent further testing in FCM to evaluate their efficacy in inhibiting H3 binding to CHO-K1 cell surfaces. AI-PoxBlock723 stood out, significantly reducing H3 binding at a concentration of 10 μM, while the other inhibitors displayed no tendency to inhibit H3 binding to HS on cell surfaces (**Fig. 5B**, Fig. S13). Further analysis using biolayer interferometry (BLI) confirmed that AI-PoxBlock723 binds to H3 with an equilibrium dissociation constant (K_D) of 9 μM (**Fig. 5C**). To ensure specificity, we also assessed the interaction between AI-PoxBlock723 and a truncated version of H3 (residues 1-239), lacking the α-helical domain. BLI results indicated a marked reduction in binding, reinforcing the specificity of AI-PoxBlock723 for the helical domain (Fig. S14). Circular Dichroism spectroscopy also confirmed that AI-PoxBlock723 predominantly consists of α-helices, consistent with its design specifications (Fig. S15).

To evaluate the antiviral activity of AI-PoxBlocks, the inhibitors were serially diluted and incubated with the clade II MPXV isolate SZTH42 before infecting Vero E6 cells. After overnight culture, virus infection foci were determined as previously described.[52] Notably, AI-PoxBlock723 showed an antiviral effect with the half maximal inhibitory concentration (IC_{50}) of 88.6 μM, whereas other AI-PoxBlocks exhibited no inhibitory efficiency (**Fig. 5D**). Given the high

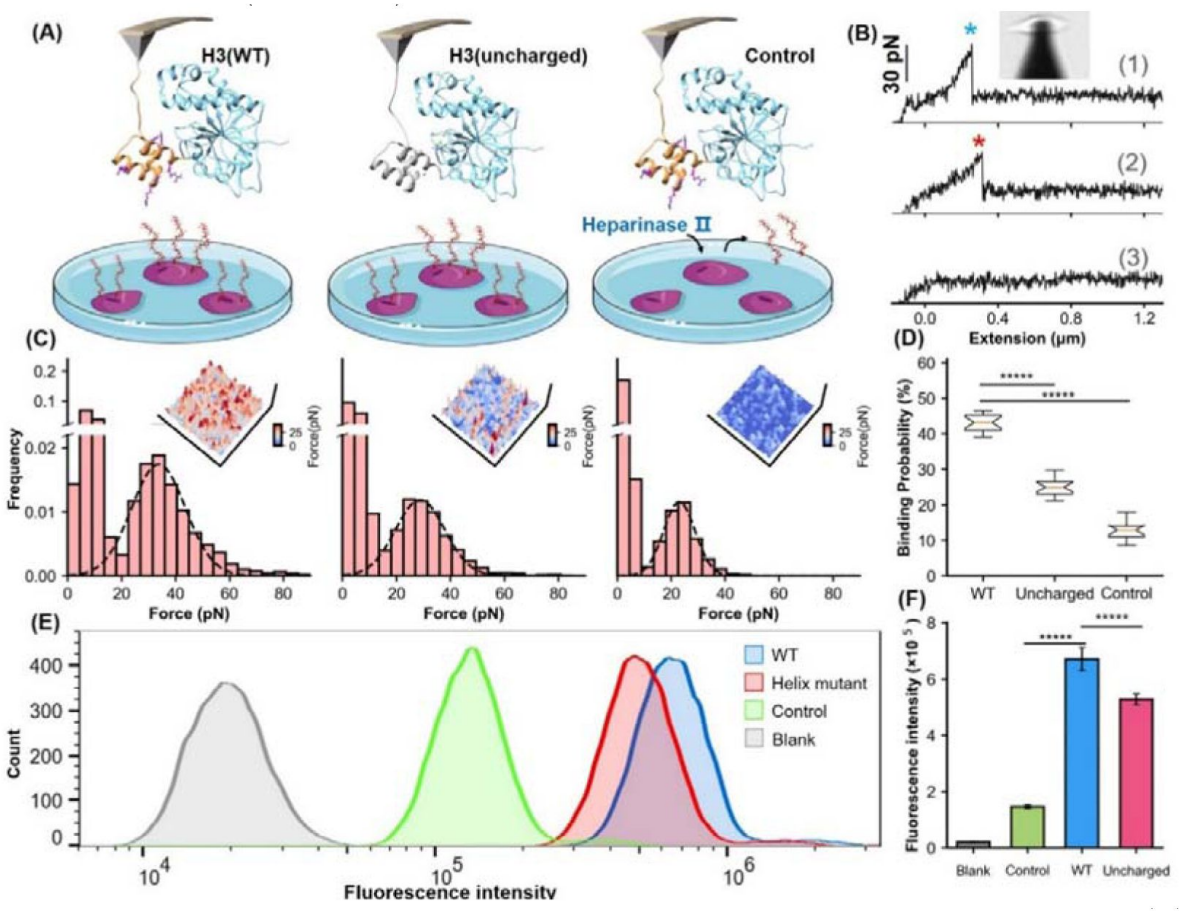

Fig. 4.

Analysis of the Helical Domain's Interaction with HS at Cellular Level

(A) Schematic of the cell force spectroscopy experiment setup shows three scenarios: wild-type H3 on an AFM tip interacting with HS on CHO-K1 cells, mutation of all basic amino acids in the H3 helical region to serine, and cells treated with HS hydrolase to remove surface HS before testing. (B) Force-extension curves depict interactions for the wild type, mutant, and control groups, marked with blue and red asterisks for dissociation events. An inset shows the optical microscope positioning the AFM probe. (C) Histograms of dissociation signals comparing the wild type, mutant, and control groups, with an inset detailing the surface distribution of dissociation forces. (D) Statistical graph showing binding probabilities for different groups, highlighting significant differences determined by t-tests ($p<1e-5$). (E) FCM results illustrate interactions of wild-type (WT) and Uncharged H3 fused with eGFP with CHO-K1 cells, alongside GFP control (green) and cell-only control (Blank, grey). (F) Statistical analysis of FCM data, showing significant differences between groups as determined by t-tests. *****, P<1e-5

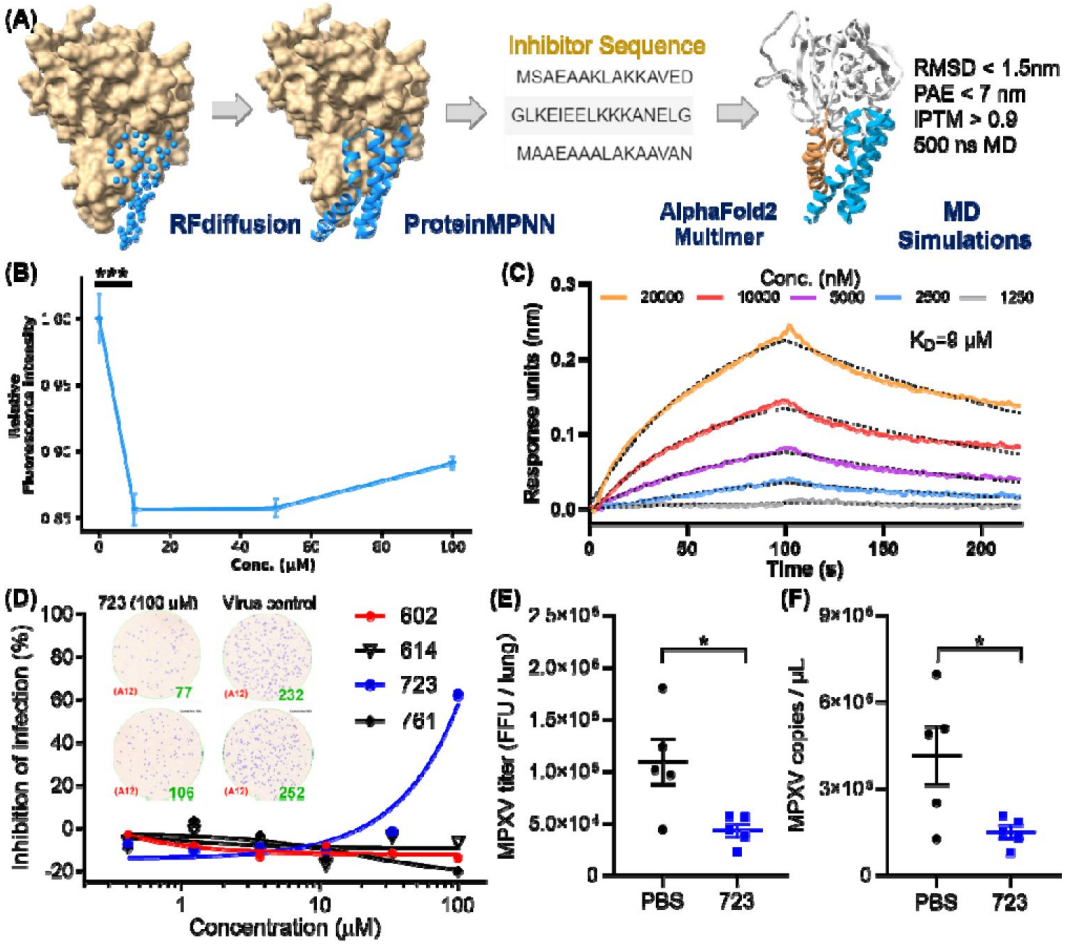

Fig. 5.

Inhibitor Design Targeting the H3-HS Interaction and Efficacy of AI-PoxBlock723

(A) Diagrams depict protein inhibitors designed to target the H3 helical region, created using RFdiffusion. Sequences capable of folding into the target scaffold structures were generated using ProteinMPNN, and were validated through AF2, followed by 500 ns MD simulations for structural stability and interaction scoring. (B) FCM analysis demonstrates the inhibitory effect of AI-Poxblock723 at various concentrations (0, 10, 50 and 100 μM, *x* axis). The control group consisted of 2 μM H3-eGFP without the inhibitor, with the relative fluorescence intensity normalized to 1. (C) BLI confirms direct interaction between AI-Poxblock723 and the H3 helical domain. (D) Graphs display the inhibitory effect of the indicated AI-Poxblocks on MPXV infection of Vero E6 cells, with quantitative analysis of virus-infected foci provided on the right. (E-F) BALB/c mice were infected intranasally with 4×10^5 FFU MPXV and treated with single dose of AI-PoxBlock723 (10 mg/kg) or PBS immediately after challenge ($n = 5$). Infectious MPXV particles and MPXV viral loads in mice lungs at 4 dpi were determined by focus-forming assay (E) and qPCR (F).

conservation of the H3 helical domain across the four *orthopoxviruses* pathogenic to humans (Fig. S16), we also assessed AI-PoxBlock activity against VACV infection. Consistently, AI-PoxBlock723 is also effective for inhibiting VACA infection in vitro with a similar IC50 of 86.7 μM (Fig. S17), suggesting the helical domain as a universal antiviral target for *orthopoxvirus*.

To evaluate the efficacy of AI-PoxBlock723 in vivo, groups of BALB/c mice were challenged with 4×10^5 FFU (focus forming unit) MPXV/SZTH42 as we previously reported[53]. Mice were administered intraperitoneally with single dose of AI-PoxBlock723 (10 mg/kg) or PBS immediately after MPXV challenge, and were sacrificed 4 days post-infection (dpi) for the determination of pulmonary MPXV titers. The MPXV infectious particles and genome copies in lungs of the AI-PoxBlock723 treated mice were significantly lower than that in the control mice (**Fig. 5E-F**, Fig. S18).

These results demonstrate the efficacy of the designed inhibitors targeting the H3 helical domain and validate the crucial role of this domain in viral adhesion, providing a promising foundation for the development of novel antiviral agents.

Discussion

Our study provides new mechanistic insights into MPXV infection by identifying the α-helical domain of the H3 protein as a critical mediator of heparan sulfate (HS) binding. This domain, previously uncharacterized, plays a pivotal role in viral adhesion to host cells, a key step in MPXV pathogenesis. Using a combination of AI-based tools and molecular dynamics (MD) simulations, we successfully identified the specific interaction sites between H3 and HS, offering a novel target for antiviral drug design[54].

Previous studies have highlighted the importance of viral adhesion proteins in *orthopoxvirus* infection, but the specific mechanisms underlying the H3-HS interaction remained unresolved. Our findings provide the first detailed structural insight into this interaction, confirming the importance of the electrostatic nature of H3-HS binding. These results align with prior reports indicating the role of HS in viral entry, but advance the field by identifying specific residues within the α-helical domain that are crucial for binding.

One of the strengths of this study lies in the application of advanced AI-based tools, such as AlphaFold2 and RFdiffusion, alongside MD simulations. These cutting-edge computational approaches allowed us to overcome the limitations imposed by the dynamic and flexible nature of HS. In addition, HS serves as a cellular ligand for various viruses[55-57], underscoring the importance of studying its interactions with viral adhesion proteins. By predicting the structure-function relationship of the H3-HS interaction, we were able to pinpoint key binding residues and mechanisms that were previously inaccessible. This demonstrates the growing potential of AI in structural biology, particularly for the complex protein-glycan interactions[56, 58,59].

The identification of the α-helical domain in H3 as a key player in HS binding offers a promising new target for antiviral drug development[17, 60-67]. Given the conservation of this domain across *orthopoxviruses*, including variola and vaccinia viruses, targeting this region could lead to the development of broad-spectrum antivirals effective against multiple *orthopoxviruses*[68]. Our study highlights the power of AI-driven drug design, as demonstrated by the promising results of AI-PoxBlock723, which showed efficacy in inhibiting viral infection. Further optimization and testing of these inhibitors in clinical models will be critical steps toward developing effective antiviral therapies. For example, conjugate the peptides with carrier molecules, such as liposomes, nanoparticles, or dendrimers, which can protect the peptides from immune detection and improve their delivery to target cells.

Looking ahead, the methodologies and findings from this study are likely to catalyze further investigations into viral adhesion mechanisms, not only in *orthopoxviruses* but also across other viral families that utilize similar adhesion strategies. Although challenges remain, we hope our discovery will attract structural biologists to resolve this domain's structure in H3, and even the structure of H3-HS complex, to further enhance drug design efficiency for this target. Although this domain itself cannot express, we chemically synthesized it (residues 240-279). CD measurement on this fragment indeed showed an α-helical structure (Fig. S19). As AIdriven approaches continue to evolve, they are poised to play a transformative role in advancing our understanding of viral pathogenesis and revolutionizing the future of drug discovery.

Acknowledgements

We appreciate the inspiring comments from previous anonymous reviewers. We acknowledge the funding support from the National Natural Science Foundation of China (22222703, 22477058), the Fundamental Research Funds for the Central Universities (020514380335), the Natural Science Foundation of Jiangsu Province (BK20202004), Shenzhen Medical Research Funds (B2302052). The numerical calculations in this work have been done on the computing facilities in the High-Performance Computing Center (HPCC) of Nanjing University.

Additional information

Author contributions

Conceptualization: PZ

Investigation: BZ, MD, YX, JQ, SW, RG, GT, LC

Funding acquisition: PZ, LC

Project administration & Supervision: PZ

Writing – original draft: PZ, BZ, LC

Competing interests

The authors declare no competing interests.

Data and materials availability

All data are available in the main text or the supplementary materials

References

1. Lum F.-M., Torres-Ruesta A., Tay M. Z., Lin R. T. P., Lye D. C., Renia L., Ng L. F. P. (2022) **Monkeypox: disease epidemiology, host immunity and clinical interventions** *Nat. Rev. Immunol* **22**:597–613

2. D. The Lancet Infectious (2022) **Monkeypox: a neglected old foe** *Lancet Infect. Dis* **22**

3. Otoole A. *et al.* (2023) **APOBEC3 deaminase editing in mpox virus as evidence for sustained human transmission since at least 2016** *Science* **382**:595–600

4. Kirby T. (2023) **What happened to the mpox pandemic?** *The Lancet* **402**:949–950

5. Vakaniaki E. H. *et al.* (2024) **Sustained human outbreak of a new MPXV clade I lineage in eastern Democratic Republic of the Congo** *Nature Medicine* https://doi.org/10.1038/s41591-024-03130-3

6. Li P. *et al.* (2023) **Mpox virus infection and drug treatment modelled in human skin organoids** *Nat. Microbiol* **8**:2067–2079

7. Liu J. *et al.* (2022) **Retrospective detection of monkeypox virus in the testes of nonhuman primate survivors** *Nat. Microbiol* **7**:1980–1986

8. Zahmatyar M. *et al.* (2023) **Human monkeypox: history, presentations, transmission, epidemiology, diagnosis, treatment, and prevention** *Front. Med* **10**

9. Zaeck L. M. *et al.* (2023) **Low levels of monkeypox virus-neutralizing antibodies after MVA-BN vaccination in healthy individuals** *Nat. Med* **29**:270–278

10. Yu J. *et al.* (2023) **Phylogeny and molecular evolution of the first local monkeypox virus cluster in Guangdong Province, China** *Nat. Commun* **14**

11. Peng Q., Xie Y., Kuai L., Wang H., Qi J., Gao G. F., Shi Y. (2023) **Structure of monkeypox virus DNA polymerase holoenzyme** *Science* **379**:100–105

12. Moss B. (2020) **Investigating Viruses During the Transformation of Molecular Biology: Part II** *Annu. Rev. Virol* **7**:15–36

13. Gray R. D. M., Albrecht D., Beerli C., Huttunen M., Cohen G. H., White I. J., Burden J. J., Henriques R., Mercer J. (2019) **Nanoscale polarization of the entry fusion complex of vaccinia virus drives efficient fusion** *Nat. Microbiol* **4**:1636–1644

14. Fonseca F. G. d., Wolffe E. J., Weisberg A., Moss B. (2000) **Effects of Deletion or Stringent Repression of the H3L Envelope Gene on Vaccinia Virus Replication** *J. Virol* **74**:7518–7528

15. Crickard L., Babas T., Seth S., Silvera P., Koriazova L., Crotty S. (2012) **Protection of Rabbits and Immunodeficient Mice against Lethal Poxvirus Infections by Human Monoclonal Antibodies** *Plos One* **7**

16. Zuiani A. *et al.* (2024) **A multivalent mRNA monkeypox virus vaccine (BNT166) protects mice and macaques from orthopoxvirus disease** *Cell* **187**:1363–1373

17. Gulati P., Chadha J., Harjai K., Singh S. (2023) **Targeting envelope proteins of poxviruses to repurpose phytochemicals against monkeypox: An in silico investigation** *Front. Microbiol* **13**

18. Jumper J. *et al.* (2021) **Highly accurate protein structure prediction with AlphaFold** *Nature* **596**:583–589

19. Phillips J. C., Braun R., Wang W., Gumbart J., Tajkhorshid E., Villa E., Chipot C., Skeel R. D., Kale L., Schulten K. (2005) **Scalable molecular dynamics with NAMD** *J. Comput. Chem* **26**:1781–1802

20. Gräter F., Shen J., Jiang H., Gautel M., Grubmuller H. (2005) **Mechanically Induced Titin Kinase Activation Studied by Force-Probe Molecular Dynamics Simulations** *Biophy. J* **88**:790–804

21. Kim E., Lee S., Jeon A., Choi J. M., Lee H.-S., Hohng S., Kim H.-S. (2013) **A single-molecule dissection of ligand binding to a protein with intrinsic dynamics** *Nat. Chem. Biol* **9**:313–318

22. Brooks C. L., MacKerell A. D., Post C. B., Nilsson L. (2024) **Biomolecular dynamics in the 21st century** *Biochim. Biophys. Acta. Gen. Subj* **1868**

23. Rief M., Gautel M., Oesterhelt F., Fernandez J. M., Gaub H. E. (1997) **Reversible unfolding of individual titin immunoglobulin domains by AFM** *Science* **276**:1109–1112

24. Sieben C., Kappel C., Zhu R., Wozniak A., Rankl C., Hinterdorfer P., Grubmuller H., Herrmann A. (2012) **Influenza virus binds its host cell using multiple dynamic interactions** *Proc. Natl. Acad. Sci. U. S. A* **109**:13626–13631

25. Raab A., Han W., Badt D., Smith-Gill S. J., Lindsay S. M., Schindler H., Hinterdorfer P. (1999) **Antibody recognition imaging by force microscopy** *Nat. Biotech* **17**

26. Muller D. J., Helenius J., Alsteens D., Dufrene Y. F. (2009) **Force probing surfaces of living cells to molecular resolution** *Nat. Chem. Biol* **5**:383–390

27. Dauparas J. *et al.* (2022) **Robust deep learning-based protein sequence design using ProteinMPNN** *Science* **378**:49–56

28. Watson J. L. *et al.* (2023) **De novo design of protein structure and function with RFdiffusion** *Nature* **620**:1089–1100

29. Singh K., Gittis A. G., Gitti R. K., Ostazeski S. A., Su H.-P., Garboczi D. N. (2016) **The Vaccinia Virus H3 Envelope Protein, a Major Target of Neutralizing Antibodies, Exhibits a Glycosyltransferase Fold and Binds UDP-Glucose** *J. Virol* **90**:5020–5030

30. Fonseca F. G. d., Wolffe E. J., Weisberg A., Moss B. (2000) **Characterization of the Vaccinia Virus H3L Envelope Protein: Topology and Posttranslational Membrane Insertion via the C-Terminal Hydrophobic Tail** *J. Virol* **74**:7508–7517

31. Lin C.-L., Chung C.-S., Heine H. G., Chang W. (2000) **Vaccinia Virus Envelope H3L Protein Binds to Cell Surface Heparan Sulfate and Is Important for Intracellular Mature Virion Morphogenesis and Virus Infection In Vitro and In Vivo** *J. Virol* **74**:3353–3365

32. Morgan A., Wang X. (2013) **The Novel Heparin-Binding Motif in Decorin-Binding Protein A from Strain B31 of Borrelia burgdorferi Explains the Higher Binding Affinity** *Biochemistry-Us* **52**:8237–8245

33. Lin Z. *et al.* (2023) **Evolutionary-scale prediction of atomic-level protein structure with a language model** *Science* **379**:1123–1130

34. Baek M., McHugh R., Anishchenko I., Jiang H., Baker D., DiMaio F. (2024) **Accurate prediction of protein-nucleic acid complexes using RoseTTAFoldNA** *Nature Methods* **21**:117–121

35. Eberhardt J., Santos-Martins D., Tillack A. F., Forli S. (2021) **AutoDock Vina 1.2.0: New Docking Methods, Expanded Force Field, and Python Bindings** *J. Chem. Inf. Model* **61**:3891–3898

36. Lee J. *et al.* (2015) **CHARMM-GUI Input Generator for NAMD, GROMACS, AMBER, OpenMM, and CHARMM/OpenMM Simulations Using the CHARMM36 Additive Force Field** *J. Chem. Theory Comput* **12**:405–413

37. Sugita Y., Okamoto Y. (1999) **Replica-exchange molecular dynamics method for protein folding** *Chem. Phys. Lett* **314**:141–151

38. Kumar V. Govind, Polasa A., Agrawal S., Kumar T. K. S., Moradi M. (2022) **Binding affinity estimation from restrained umbrella sampling simulations** *Nat. Comput. Sci* **3**:59–70

39. Altschul S. F., Madden T. L., Schaffer A. A., Zhang J. H., Zhang Z., Miller W., Lipman D. J. (1997) **Gapped BLAST and PSI-BLAST: a new generation of protein database search programs** *Nucleic Acids Res* **25**:3389–3402

40. Yu H., Siewny M. G. W., Edwards D. T., Sanders A. W., Perkins T. T. (2017) **Hidden dynamics in the unfolding of individual bacteriorhodopsin proteins** *Science* **355**:945–950

41. Dietz H., Rief M. (2004) **Exploring the energy landscape of GFP by single-molecule mechanical experiments** *Proc. Natl. Acad. Sci. U. S. A* **101**:16192–16197

42. Goktas M., Luo C. F., Sullan R. M. A., Bergues-Pupo A. E., Lipowsky R., Verde A. V., Blank K. G. (2018) **Molecular mechanics of coiled coils loaded in the shear geometry** *Chem. Sci* **9**:4610–4621

43. Cao Y., Lam C., Wang M., Li H. (2006) **Nonmechanical protein can have significant mechanical stability** *Angew. Chem. Int. Ed* **45**:642–645

44. Stahl S. W., Nash M. A., Fried D. B., Slutzki M., Barak Y., Bayer E. A., Gaub H. E. (2012) **Single-molecule dissection of the high-affinity cohesin-dockerin complex** *Proc. Natl. Acad. Sci. U. S. A* **109**:20431–20436

45. Zheng B., Xiao Y., Tong B., Mao Y., Ge R., Tian F., Dong X., Zheng P. (2023) **S373P Mutation Stabilizes the Receptor-Binding Domain of the Spike Protein in Omicron and Promotes Binding** *JACS Au* **3**:1902–1910

46. Shi S., Wang Z., Deng Y., Tian F., Wu Q., Zheng P. (2022) **Combination of Click Chemistry and Enzymatic Ligation for Stable and Efficient Protein Immobilization for Single-Molecule Force Spectroscopy** *CCS Chem* **4**:598–604

47. Deng Y., Wu T., Wang M., Shi S., Yuan G., Li X., Chong H., Wu B., Zheng P. (2019) **Enzymatic biosynthesis and immobilization of polyprotein verified at the single-molecule level** *Nat. Commun* **10**:2775–2785

48. Liu Y., Song D., Li S., Guo Z., Zheng P. (2024) **Click Chemistry-Based Force Spectroscopy Revealed Enhanced Binding Dynamics of Phosphorylated HMGB1 to Cisplatin-DNA** *J. Am. Chem. Soc* **146**:13126–13132

49. Carrion-Vazquez M., Oberhauser A. F., Fowler S. B., Marszalek P. E., Broedel S. E., Clarke J., Fernandez J. M. (1999) **Mechanical and chemical unfolding of a single protein: A comparison** *Proc. Natl. Acad. Sci. U. S. A* **96**:3694–3699

50. Tian F., Tong B., Sun L., Shi S., Zheng B., Wang Z., Dong X., Zheng P. (2021) **N501Y mutation of spike protein in SARS-CoV-2 strengthens its binding to receptor ACE2** *Elife* **10**

51. Alsteens D., Newton R., Schubert R., Martinez-Martin D., Delguste M., Roska B., Muller D. J. (2016) **Nanomechanical mapping of first binding steps of a virus to animal cells** *Nat. Nanotechnol* **12**

52. Cheng L., Yang L., Wang M., Peng Y., Wang H., Yang X., Zhao J., Zhang M., Wang F., Zhang Z. (2024) **Isolation and characterization of mpox virus from the first mpox case in Shenzhen, China** *Virologica Sinica* **39**:335–337

53. Cheng L., Huang W., Duan M., Li Z., Chen Q., Zhang M., Zhang Z. (2024) **Pathogenic BALB/c mice infection model for evaluation of mpox countermeasures** *Cell Discovery* **10**

54. Monzon S. *et al.* (2024) **Monkeypox virus genomic accordion strategies** *Nat. Commun* **15**

55. Clausen T. M. *et al.* (2020) **SARS-CoV-2 Infection Depends on Cellular Heparan Sulfate and ACE2** *Cell* **183**:1043–1057

56. Shriver Z., Capila I., Venkataraman G., Sasisekharan R., Lever R., Mulloy B., Page C. P. (2012) **Heparin and Heparan Sulfate: Analyzing Structure and Microheterogeneity** *Heparin - A Century of Progress* Berlin, Heidelberg: Springer Berlin Heidelberg :159–176 https://doi.org/10.1007/978-3-642-23056-1_8

57. Koehler M., Delguste M., Sieben C., Gillet L., Alsteens D. (2020) **Initial Step of Virus Entry: Virion Binding to Cell-Surface Glycans** *Annu. Rev. Virol* **7**:143–165

58. Shih P.-C., Yang M.-S., Lin S.-C., Ho Y., Hsiao J.-C., Wang D.-R., Yu S. S. F., Chang W., Tzou D.-L. M. (2009) **A Turn-like Structure "KKPE" Segment Mediates the Specific Binding of Viral Protein A27 to Heparin and Heparan Sulfate on Cell Surfaces** *J. Bio. Chem* **284**:36535–36546

59. Marszalek P. E., Oberhauser A. F., Li H., Fernandez J. M. (2003) **The Force-Driven Conformations of Heparin Studied with Single Molecule Force Microscopy** *Biophy. J* **85**:2696–2704

60. Zhang Z. Q., Xie J., Liu H. Y., Liu J., Linhardt R. J. (2009) **Quantification of Heparan Sulfate Disaccharides Using Ion-Pairing Reversed-Phase Microflow High-Performance Liquid Chromatography with Electrospray Ionization Trap Mass Spectrometry** *Anal. Chem* **81**:4349–4355

61. Podduturi S., Vemula D., Singothu S., Bhandari V. (2023) **In-silico investigation of E8 surface protein of the monkeypox virus to identify potential therapeutic agents** *J. Biomol. Struct. Dyn* :1–14 https://doi.org/10.1080/07391102.2023.2245041

62. Bernardi R. C., Durner E., Schoeler C., Malinowska K. H., Carvalho B. G., Bayer E. A., Luthey-Schulten Z., Gaub H. E., Nash M. A. (2019) **Mechanisms of Nanonewton Mechanostability in a Protein Complex Revealed by Molecular Dynamics Simulations and Single-Molecule Force Spectroscopy** *J. Am. Chem. Soc* **141**:14752–14763

63. Zhao M., Woodside M. T. (2021) **Mechanical strength of RNA knot in Zika virus protects against cellular defenses** *Nat. Chem. Biol* **17**:975–981

64. Serdiuk T., Balasubramaniam D., Sugihara J., Mari S. A., Kaback H. R., Müller D.J. (2016) **YidC assists the stepwise and stochastic folding of membrane proteins** *Nat. Chem. Biol* **12**:911–917

65. Gupta P. S. Sen, Panda S. K., Nayak A. K., Rana M. K. (2023) **Identification and Investigation of a Cryptic Binding Pocket of the P37 Envelope Protein of Monkeypox Virus by Molecular Dynamics Simulations** *J. Phys. Chem. Lett* **14**:3230–3235

66. Petrosyan R., Patra S., Rezajooei N., Garen C. R., Woodside M. T. (2021) **Unfolded and intermediate states of PrP play a key role in the mechanism of action of an antiprion chaperone** *Proc. Natl. Acad. Sci. U. S. A* **118**

67. Chen G., Wang H., Bumba L., Masin J., Sebo P., Li H. (2023) **The adenylate cyclase toxin RTX domain follows a series templated folding mechanism with implications for toxin activity** *J. Biol. Chem* **299**

68. Wang J., Shahed-Ai-Mahmud M., Chen A., Li K., Tan H., Joyce R. (2023) **An Overview of Antivirals against Monkeypox Virus and Other Orthopoxviruses** *J. Med. Chem* **66**:4468–4490

Author information

Bin Zheng[#]
State Key Laboratory of Coordination Chemistry, Chemistry and Biomedicine Innovation Center (ChemBIC), School of Chemistry and Chemical Engineering, Nanjing University, Nanjing, China
ORCID iD: 0000-0002-0721-7099

[#]These authors contributed equally to this work

Meimei Duan[#]
Institute for Hepatology, National Clinical Research Center for Infectious Disease, Shenzhen Third People's Hospital, Shenzhen, China

[#]These authors contributed equally to this work

Yifen Huang[#]
State Key Laboratory of Coordination Chemistry, Chemistry and Biomedicine Innovation Center (ChemBIC), School of Chemistry and Chemical Engineering, Nanjing University, Nanjing, China

[#]These authors contributed equally to this work

Shangchen Wang[#]
State Key Laboratory of Coordination Chemistry, Chemistry and Biomedicine Innovation Center (ChemBIC), School of Chemistry and Chemical Engineering, Nanjing University, Nanjing, China

[#]These authors contributed equally to this work

Jun Qiu
State Key Laboratory of Coordination Chemistry, Chemistry and Biomedicine Innovation Center (ChemBIC), School of Chemistry and Chemical Engineering, Nanjing University, Nanjing, China

Zhuojian Lu
State Key Laboratory of Coordination Chemistry, Chemistry and Biomedicine Innovation Center (ChemBIC), School of Chemistry and Chemical Engineering, Nanjing University, Nanjing, China

Lichao Liu
State Key Laboratory of Coordination Chemistry, Chemistry and Biomedicine Innovation Center (ChemBIC), School of Chemistry and Chemical Engineering, Nanjing University, Nanjing, China

Guojin Tang
State Key Laboratory of Coordination Chemistry, Chemistry and Biomedicine Innovation Center (ChemBIC), School of Chemistry and Chemical Engineering, Nanjing University, Nanjing, China

Lin Cheng
Institute for Hepatology, National Clinical Research Center for Infectious Disease, Shenzhen Third People's Hospital, Shenzhen, China

For correspondence: chenglin252@163.com

Peng Zheng
State Key Laboratory of Coordination Chemistry, Chemistry and Biomedicine Innovation Center (ChemBIC), School of Chemistry and Chemical Engineering, Nanjing University, Nanjing, China, Department of Intensive Care Unit, Nanjing Drum Tower Hospital, Affiliated Hospital of Medical School, Nanjing University, Nanjing, China
ORCID iD: 0000-0003-4792-6364

For correspondence: pengz@nju.edu.cn

Editors

Reviewing Editor
Juan Ludert
Center for Research and Advanced Studies (CINVESTAV), Mexico City, Mexico

Senior Editor
Volker Dötsch
Goethe University Frankfurt, Frankfurt am Main, Germany

Reviewer #1 (Public Review):

Summary:

The study aimed to better understand the role of the H3 protein of the Monkeypox virus (MPXV) in host cell adhesion, identifying a crucial α-helical domain for interaction with heparan sulfate (HS). Using a combination of advanced computational simulations and experimental validations, the authors discovered that this domain is essential for viral adhesion and potentially a new target for developing antiviral therapies.

Strengths:

The study's main strengths include the use of cutting-edge computational tools such as AlphaFold2 and molecular dynamics simulations, combined with robust experimental techniques like single-molecule force spectroscopy and flow cytometry. These methods provided a detailed and reliable view of the interactions between the H3 protein and HS. The study also highlighted the importance of the α-helical domain's electric charge and the influence of the Mg(II) ion in stabilizing this interaction. The work's impact on the field is significant, offering new perspectives for developing antiviral treatments for MPXV and potentially other viruses with similar adhesion mechanisms. The provided methods and data are highly useful for researchers working with viral proteins and protein-polysaccharide interactions, offering a solid foundation for future investigations and therapeutic innovations.

Comments on revised version:

The authors have successfully addressed the questions raised in my review.

https://doi.org/10.7554/eLife.100545.2.sa3

Reviewer #2 (Public Review):

Summary:

The manuscript presenting the discovery of a heparan-sulfate (HS) binding domain in monkeypox virus (MPXV) H3 protein as a new anti-poxviral drug target, presented by Bin Zhen and co-workers, is of interest, given that it offers a potentially broad antiviral substance to be used against poxviruses. Using new computational biology techniques, the authors identified a new alpha-helical domain in the H3 protein, which interacts with cell surface HS, and this domain seems to be crucial for H3-HS interaction. Given that this domain is conserved across orthopoxviruses, authors designed protein inhibitors. One of these inhibitors, AI-PoxBlock723, effectively disrupted the H3-HS interaction and inhibited infection with Monkeypox virus and Vaccinia virus. The presented data should be of interest to a diverse audience, given the possibility of an effective anti-poxviral drug.

Strengths:

In my opinion, the experiments done in this work were well-planned and executed. The authors put together several computational methods, to design poxvirus inhibitor molecules, and then they test these molecules for infection inhibition.

Comments on revised version:

The authors have addressed the comments I made in my review.

https://doi.org/10.7554/eLife.100545.2.sa2

Reviewer #3 (Public Review):

Summary:

The article is an interesting approach to determining the MPOX receptor using "in silico" tools. The results show the presence of two regions of the H3 protein with a high probability of being involved in the interaction with the HS cell receptor. However, the α-helical region seems to be the most probable, since modifications in this region affect the virus binding to the HS receptor.

Strengths:

In my opinion, it is an informative article with interesting results, generated by a combination of "in silico" and wet science to test the theoretical results. This is a strong point of the article.

Comments on revised version:

After a review of the changes to the manuscript and the author's responses, no further changes are needed.

https://doi.org/10.7554/eLife.100545.2.sa1

Author response:

The following is the authors' response to the original reviews.

> ***Public Reviews:***
>
> ***Reviewer #1 (Public Review):***
>
> *Summary:*
>
> *The study aimed to better understand the role of the H3 protein of the Monkeypox virus (MPXV) in host cell adhesion, identifying a crucial α-helical domain for interaction with heparan sulfate (HS). Using a combination of advanced computational simulations and experimental validations, the authors discovered that this domain is essential for viral adhesion and potentially a new target for developing antiviral therapies.*
>
> *Strengths:*
>
> *The study's main strengths include the use of cutting-edge computational tools such as AlphaFold2 and molecular dynamics simulations, combined with robust experimental techniques like single-molecule force spectroscopy and flow cytometry. These methods*

> *provided a detailed and reliable view of the interactions between the H3 protein and HS. The study also highlighted the importance of the α-helical domain's electric charge and the influence of the Mg(II) ion in stabilizing this interaction. The work's impact on the field is significant, offering new perspectives for developing antiviral treatments for MPXV and potentially other viruses with similar adhesion mechanisms. The provided methods and data are highly useful for researchers working with viral proteins and protein-polysaccharide interactions, offering a solid foundation for future investigations and therapeutic innovations.*
>
> *Weaknesses:*
>
> *However, some limitations are notable. Despite the robust use of computational methodologies, the limitations of this approach are not discussed, such as potential sources of error, standard deviation rates, and known controls for the H3 protein to justify the claims. Additionally, validations with methodologies like X-ray crystallography would further benefit the visualization of the H3 and HS interaction.*

Thank you very much for the evaluation and appreciation of our work. In response to the identified weakness, we have conducted additional analyses to further assess the limitations of the computational methodologies used. Specifically, we predicted the MPXV H3 structure using two other AI-based protein structure prediction models, ESMFold and RoseTTAFold2. Both models also predicted an a-helical structure, which supports our conclusion. However, they yielded lower pLDDT scores (Figure S1A-C in the revised SI), indicating that some error may be present.

We agree with this reviewer, as well as the other reviewers, that X-ray crystallography data for the H3 structure would be highly valuable. Unfortunately, we lack the expertise in structural biology to obtain these results at this stage. To complement this, we performed molecular dynamics (MD) simulations, which suggest that the helical domain is connected to the main domain via a flexible linker. This flexibility may help explain the challenges in obtaining a high-resolution X-ray structure. In fact, to date, the only structural data available for H3 is from the VAVC, which excludes the helical domain (The helical domain part is cleaved for the X-ray studies). We have added this point to the discussion and hope that experts in structural biology will be able to resolve the structure of this domain in the future.

> ***Reviewer #2 (Public Review):***
>
> *Summary:*
>
> *The manuscript presenting the discovery of a heparan-sulfate (HS) binding domain in monkeypox virus (MPXV) H3 protein as a new anti-poxviral drug target, presented by Bin Zhen and co-workers, is of interest, given that it offers a potentially broad antiviral substance to be used against poxviruses. Using new computational biology techniques, the authors identified a new alpha-helical domain in the H3 protein, which interacts with cell surface HS, and this domain seems to be crucial for H3-HS interaction. Given that this domain is conserved across orthopoxviruses, authors designed protein inhibitors. One of these inhibitors, AI-PoxBlock723, effectively disrupted the H3-HS interaction and inhibited infection with Monkeypox virus and Vaccinia virus. The presented data should be of interest to a diverse audience, given the possibility of an effective anti-poxviral drug.*
>
> *Strengths:*
>
> *In my opinion, the experiments done in this work were well-planned and executed. The authors put together several computational methods, to design poxvirus inhibitor molecules, and then they test these molecules for infection inhibition.*
>
> *Weaknesses:*

> *One thing that could be improved, is the presentation of results, to make them more easily understandable to readers, who may not be experts in protein modeling programs. For example, figures should be self-explanatory and understood on their own, without the need to revise text. Therefore, the figure legend should be more informative as to how the experiments were done.*

Thank you very much for your appreciation of our work and your support. In response to the identified weakness, we have carefully reviewed all the figure legends to ensure they are more informative.

> ***Reviewer #3 (Public Review):***
>
> *Summary:*
>
> *The article is an interesting approach to determining the MPOX receptor using "in silico" tools. The results show the presence of two regions of the H3 protein with a high probability of being involved in the interaction with the HS cell receptor. However, the α-helical region seems to be the most probable, since modifications in this region affect the virus binding to the HS receptor.*
>
> *Strengths:*
>
> *In my opinion, it is an informative article with interesting results, generated by a combination of "in silico" and wet science to test the theoretical results. This is a strong point of the article.*
>
> *Weaknesses:*
>
> *Has a crystal structure of the H3 protein been reported?*
>
> *The following text is in line 104: "which may represent a novel binding site for HS". It is unclear whether this means this "new binding site" is an alternative site to an old one or whether it is the true binding site that had not been previously elucidated.*

Thank you very much for your thoughtful evaluation and appreciation of our work.

We agree with this reviewer, as well as the other reviewers, that X-ray crystallography data for the H3 structure would be highly valuable. Unfortunately, we are not experts in structural biology, and we have not yet been able to obtain these structural results. To date, the only structure available for H3 is the one from VAVC, which does not include the helical domain. We have included this point in the discussion and hope that experts in structural biology will be able to resolve the structure of this domain in the future.

Regarding the "novel binding site," this term refers to "the true binding site that had not been previously elucidated." Previous research identified that H3 binds to heparan sulfate (HS), but the exact binding site had not been determined.

> ***Recommendations for the authors:***
>
> ***Reviewer #1 (Recommendations For The Authors):***
>
> *Validation of Results with Other Experimental Methods: While single-molecule force spectroscopy and flow cytometry provide valuable data, including complementary methods such as X-ray crystallography could offer additional insights into the H3-HS interaction and the effectiveness of the inhibitors.*

> *Discussion of Computational Model Limitations: Although the use of AlphaFold2 and other advanced tools is a strength, it is important to discuss the limitations of these models in more detail, including potential sources of error and how they may impact the interpretation of the results.*
>
> *During the manuscript evaluation, it is not clear the protein localization (transmembrane?) since the proteins̀ end is very close to the virus membrane surface. All experiments demonstrated the protein without being anchored to the membrane, letting the interaction site always be exposed. If the protein is linked to the membrane, how would the site be exposed due to the limited space between it and the virus structure?*

Thank you for these insightful comments. As you pointed out, the H3 protein, particularly the helical domain at the C-terminal, is indeed located close to the membrane, which could limit the available space for H3 binding. To investigate this further, we modeled the full-length H3 protein in the context of the membrane and performed molecular dynamics (MD) simulations to assess the available space. Our results show that there is more than 1 nm of space between the helical domain and the membrane, which should be sufficient for potential heparan sulfate (HS) binding (see Figure 1E, and Figure S1D&E in the revised manuscript).

> *Minor corrections:*
>
> *Line 31: "is an emerging zoonotic pathogen" should be revised to reflect that Mpox is a re-emerging virus, given its history of causing outbreaks, such as in 2003.*
>
> *Line 71 and Line 75: Adding an explanation of "Mg binding sites" and "GAG motifs" would enhance reader understanding, as these represent important points in the study. The current positioning of Figure 1 causes some confusion for the reader.*
>
> *Line 111: High score? What controls were used for the protein? Are there known inhibitors of H3? If so, why weren't they tested for structure comparison? Additionally, what about other molecules that H3 binds to, such as UDP-Glucose, as demonstrated in the base article for the Vaccinia virus H3 protein available in the PDB?*
>
> *Figure 2B: Improve the legend, as the colors of the lines are not clear.*

Thank you for your instructive comments. We have addressed most of them in the revised manuscript.

Regarding the "high score," AlphaFold2 provides a confidence score for its protein structure predictions, with a maximum score of 100. A score above 80 indicates a high level of confidence in the prediction.

There are known inhibitors (such as antibodies) of H3, and while the sequence is available, no structure has been reported so far. Previous s NMR titration measurements have shown that UDP-glucose binds to H3, but no structural data for the complex exist. To date, the only available crystal structure is of a truncated H3, which does not include the helical domain we identified from VAVC.

> ***Reviewer #2 (Recommendations For The Authors):***
>
> *The text described in the result section does not match the text presented in Figures. So, it is not easy to see what are the authors referring to when they mention the Figure. For example, the text referring to Figure S8 mentions the GB1 domain and the Cohesin module, but these are not mentioned in Figure S8.*

> *I do not understand the results presented in Figure 5B. It is not clear to me, from the Figure legend nor after reading the Material and Methods, how this experiment was done. Specifically, what is plotted on X, is it the amount of inhibitor or the amount of protein? These things have to be checked through the manuscript.*
>
> *It would be interesting to confirm if the inhibition of infection is based on the inhibition of viral binding to the cells. This should not be complicated to realize, and it could provide evidence for the mechanism of action.*
>
> *Extensive use of terms like "this domain" is not good in this type of article, like in lines 207, and 211. It is not always clear to what domain are authors referring to, so it may be much better to mention the domain in question by the exact name.*
>
> *Line 337, If I am not mistaken dilutions are serial not series.*
>
> *Line 613, in methods. Please use g force instead of rpm, it is more informative. Even if it is just to pellet cells.*

Thank you very much for your instructive comments. We have addressed most of them in the revised manuscript. For instance, the immobilization of the GB1 domain and the cohesin module is now mentioned in Figure S9. Additionally, in the previous Figure 5B, the "x" represents the concentration of the inhibitor. Serial and g force is updated.

> ***Reviewer #3 (Recommendations For The Authors):***
>
> *Line 190*
>
> *Did you mutate all the amino acids at the same time? What was the impact of all these mutations on the structure of the helical region? Or if you modeled the protein again after replacing these 7 amino acids, did you find that there was no difference? Regardless of your answer, you must include a superposition of the mutated structure and the wt.*

Thank you for the insightful comment. We have now also predicted the structure of the serine mutant using AlphaFold2 (AF2). As expected, the helical domain structure remains largely preserved with only minor differences. We have included these results in Figure S6, as suggested.

> *Figure 2D*
>
> *In this graph, the authors should indicate the ΔG as a negative value. In fact, the graph does not match the text.*

Thanks for the reminder, it is corrected in the graph

> *Figure 4B*
>
> *Is the difference in binding force significantly different? 28.8 vs 33.7 pN*

The absolute difference in binding force is not large (~5 pN). However, for a system with a relatively low binding force, this difference is significant. Specifically, the 5 pN difference accounts for approximately a 14% reduction in binding force. We have included this percentage in the revised manuscript.

> *Figure 5*

> *If AI-PoxBlocks723 was the only peptide effective in inhibiting viral infection of MPOX and other related viruses but not with 100% effectiveness, do you think this could be a consequence of a low interaction efficiency or the existence of a different receptor? Or a secondary region of binding in the H3? Can you argue about this?*

It has been proposed that there are other adhesion proteins for MPXV, such as D8, in addition to H3. We believe this accounts for the observed less-than-100% effectiveness.

> *The use of peptides as "inhibitory tools" could have an interesting effect in vitro, however, in vivo the immunological response against the peptide will reduce/eliminate it, how you may optimize the "drug" development with this system, as you state in line 387.*

Thank you for your thoughtful comment. You are correct that the use of peptides as inhibitory tools could induce an immune response in vivo, which might limit their effectiveness over time. To optimize this approach for drug development, conjugate the peptides with carrier molecules, such as liposomes, nanoparticles, or dendrimers, which can protect the peptides from immune detection and improve their delivery to target cells. This could allow for more controlled and sustained release of the peptide in vivo, reducing the chances of immune clearance. We have added this discussion in the revised manuscript.

https://doi.org/10.7554/eLife.100545.2.sa0